

05,08

Features of nonreciprocal propagation of spin waves in a magnon crystal structure based on a bilayer film of yttrium-iron garnet with partial metallization

© A.S. Ptashenko¹, S.A. Odintsov^{1,¶}, E.H. Lock², A.V. Sadovnikov¹

¹ Saratov National Research State University, Saratov, Russia

² Fryazino Branch of Kotelnikov Institute of Radio Engineering and Electronics, Russian Academy of Sciences, Fryazino, Russia

¶ E-mail: odinoff@gmail.com

Received September 14, 2023

Revised November 14, 2023

Accepted November 17, 2023

This study investigates the spin wave spectra features in a waveguiding structure that is based on a two-layer film. The film has metal strips periodically located on one of its surfaces, forming a magnon crystal (MC). The structure is used to realize the mode of spin wave propagation in two frequency ranges for a selected value of the magnetic field. The article presents a study on the dispersion characteristics of spin waves using the finite element method. It demonstrates the formation of forbidden zones in the high-frequency range of the spectrum. By changing the configuration and location of metal strips on one side of the film, the width and position of the forbidden zones in the spectrum can be controlled. Additionally, the study shows that the properties of nonreciprocity of spin waves can be altered by changing the direction of propagation. The concept proposes a two-layer magnon-crystal structure for designing functional magnonics devices that support frequency-selective multiband modes of operation.

Keywords: magnonics, nonreciprocal systems, multilayer waveguides, magnon crystal.

DOI: 10.21883/0000000000

1. Introduction

Over many years, multilayer films based on ferromagnetic materials have been extensively studied due to continuously improved technology of magnetic layers on nonmagnetic substrates [1]. For example, magnetic thin-film structures may be represented by single, double and multilayer films consisting of various combinations of ferromagnetic (FM), antiferromagnetic (AFM) and nonmagnetic (NM) layers with various thicknesses and arrangements. FM|NM multilayer structures have been of special interest in the past decade [2].

Search for new spin-wave signal utilization methods to be used in data processing gives rise to the ideas of utilization of nonreciprocity properties for spin waves (SW) propagating in multilayer structures [1]. Yttrium-iron garnet (YIG) is the base material for magnonics due to the advanced manufacturing technology and record-low loss in SW propagation. YIG-based thin films may be used in laminar structures, e.g. YIG|metal, that make it possible to observe the appearance of the nonreciprocity effect when the SW propagation direction is reversed or the external bias field orientation is changed. Double-layer films formed from the YIG layers with various magnetization have a set of advantages compared with the YIG|metal structures due to lower propagation loss [3]. At the same time it is known that ferromagnetic film surface metallization using periodically arranged strips results in formation of band gaps (BG) in the

SW spectrum due to the occurrence of the Bragg resonance during SW propagation [4]. Whereby strong damping of SW will not be observed with partial metallization of the YIG film surface.

Study of wave-guiding structures based on double-layer YIG films is of great interest particularly for utilization as interconnecting components for functional modules of magnon networks and integration with devices intended for data signal processing using magnon-based logic [5]. Special focus in the research is made on propagation conditions in finite-width magnon microwaveguides created from multilayer ferrite films. These structures enable control of interference conditions, including the VHF input level adjustment, and are important components of Mach–Zender type interferometers [6]. It should be noted that nonlinear signal propagation conditions are possible in microwaveguides based on thin YIG films and may be studied, for example, using radiophysical methods [7–9] and the Mandelstam–Brillouin spectroscopy of magnetic materials [10–14]. In addition, the investigations are also focused on the use of multilayer films in functionality-switchable devices. For example, magnetic anisotropy switching in a multilayer structure may be achieved using external magnetic or electric fields [15]. This opens up the opportunities for creation of reprogrammable magnetoelectric devices and high density data storage memory. Multilayer films used in spin-transfer devices are also one of the interesting research areas. Such devices use the

spin transport effect when electron spins are transferred across the ferromagnetic-nonmagnetic layer interface. This opens up the opportunities for creation of energy-saving and full-speed devices for data storage and processing [16]. Tunable spin-wave devices, including phase shifters and signal switchers, based on magnon-crystalline structures are offered [17–20]. Features of SW spectra in double-layer YIG films and SW property control methods used in magnon-crystalline structures might be suitable for the design of tunable filters and magnon network components.

The study investigated the features of signal propagation in a magnonic crystal (MC) formed from a multilayer yttrium-iron garnet film with a set of metallic strips periodically arranged on the magnetic film surface. The magnetic film consists of two ferromagnetic layers with various magnetization. Various spin wave spectrum control mechanisms were studied with modification of the structure geometry. Mathematical simulation using the finite element method was conducted to study the SW spectra transformation that occurs as the effect of shift of high-frequency and low-frequency spin wave spectrum bands and band gap parameters with structure geometry variation. The findings were used to offer a concept of a double-layer spin-wave waveguide that can be utilized in controlled magnon interconnections supporting multiband operation modes.

2. Structure under study

To study the influence of metallization on the band gap position in the studied structure, we will consider a mathematical model to calculate electrodynamic performance of gyrotropic structures that are periodic in one of spatial orientations. Then we will consider a structure consisting of YIG with repetitive strips located near one of the film surfaces. Assume that the system is infinite and uniform along the x axis. For numerical simulation, the dielectric permittivity of YIG was chosen as a scalar quantity, while the magnetic permeability was described by a frequency-dependent tensor.

Using the double-layer ferrite YIG film [Y₃Fe₅O₁₂] model, we considered a double-layer microwaveguide layout whose fragment is shown in Figure 1. The double-layer film parameters were taken from [21]. One of the layers consisted of $d_1 = 6.9 \mu\text{m}$ pure YIG with a saturation magnetization of $4\pi M_1 = 1738 \text{ G}$ (YIG1) and the second layer was doped with addition of gallium and lanthanum with $d_2 = 8.9 \mu\text{m}$ and a saturation magnetization of $4\pi M_2 = 904 \text{ G}$ (YIG2). The layers were applied to a gallium-gadolinium garnet (GGG) substrate.

The microwaveguide was placed into a $H_0 = 670 \text{ Oe}$ uniform magnetic field oriented along the x axis. To form MC, $d_c = 8.9 \mu\text{m}$ periodic metallic strips were applied with spacing $L = 300 \mu\text{m}$ at a distance of $\Delta d = 1 \mu\text{m}$ from the double-layer film surface, conductivity of the metal is assumed as finite and corresponds to copper conductivity $5.998 \cdot 10^7 \text{ S/m}$. The simulation geometry constituted a

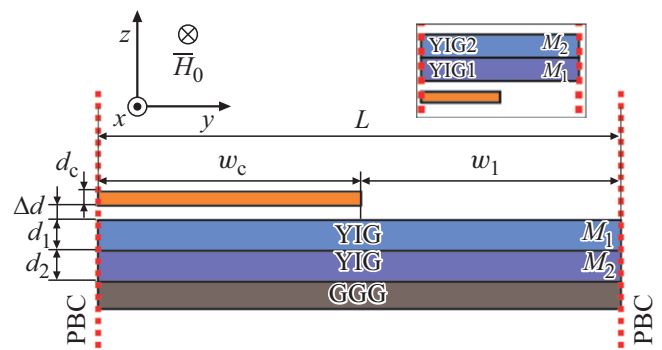


Figure 1. Diagram of the structure under study.

case of magnetostatic surface wave (MSSW) excitation tangentially to the magnetized film.

In contrast to the typical approach to the description of ferromagnetics within the magnetostatic approximation and Walker equation used for simulation of static or quasistatic magnetic fields with a known type of tensor, electrodynamic performance of MC shall be defined by means of the Maxwell equation solved for the structure shown in Figure 1 with the appropriate boundary conditions.

The Floquet periodic boundary conditions were specified on the right and left boundaries of the computational domain to ensure calculation of SW dispersion curves for the first reduced Brillouin band. They are written as follows

$$\mathbf{E}(\mathbf{x} + L, y) = \mathbf{E}(x, y) \exp(-j\beta_y L),$$

where β_y is the wave vector component along the y axis (longitudinal wave number), \mathbf{E} is the electric field strength vector.

3. Numerical simulation method

Numerical simulation and calculation of electromagnetic waves using the finite element method were carried out by solution of the Maxwell system of equations. Therefore, it is suggested that spins in the system are free, because this approach does not include the exchange interaction. Moreover, assuming that the electromagnetic field components are in harmonic dependence on frequency $e^{j\omega t}$, the second-order equation may be solved for the electric field strength vector \mathbf{E} :

$$\nabla(\mu^{-1}\nabla\mathbf{E}) - k^2\varepsilon\mathbf{E} = 0,$$

where $k = \omega/c$ is the wave number in vacuum, $\omega = 2\pi f$ is the angular frequency, f is the electromagnetic wave frequency, $\varepsilon = 14$ is the RMS dielectric permittivity for the YIG layer. The magnetic permeability tensor of each layer $\hat{\mu}_{1,2}$ was specified in the form corresponding to the electromagnetic description of the gyrotropic medium [5]:

$$\hat{\mu}_{1,2} = \begin{bmatrix} 1 & 0 & 0 \\ 0 & \mu_{1,2}(\omega) & -i\mu_{a,1,2}(\omega) \\ 0 & i\mu_{a,1,2}(\omega) & \mu_{1,2}(\omega) \end{bmatrix}$$

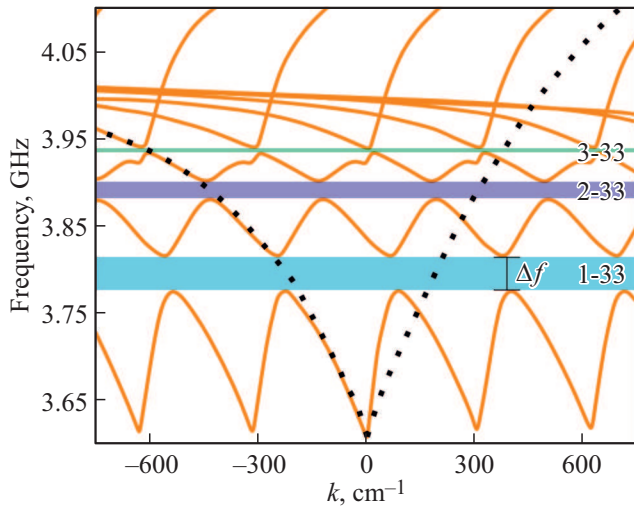


Figure 2. Dispersion curves were calculated for a structure with a $w_c = 60 \mu\text{m}$ wide copper plate (orange line) and dispersion curve calculated by solving the analytical equation from [22] (black dotted curve).

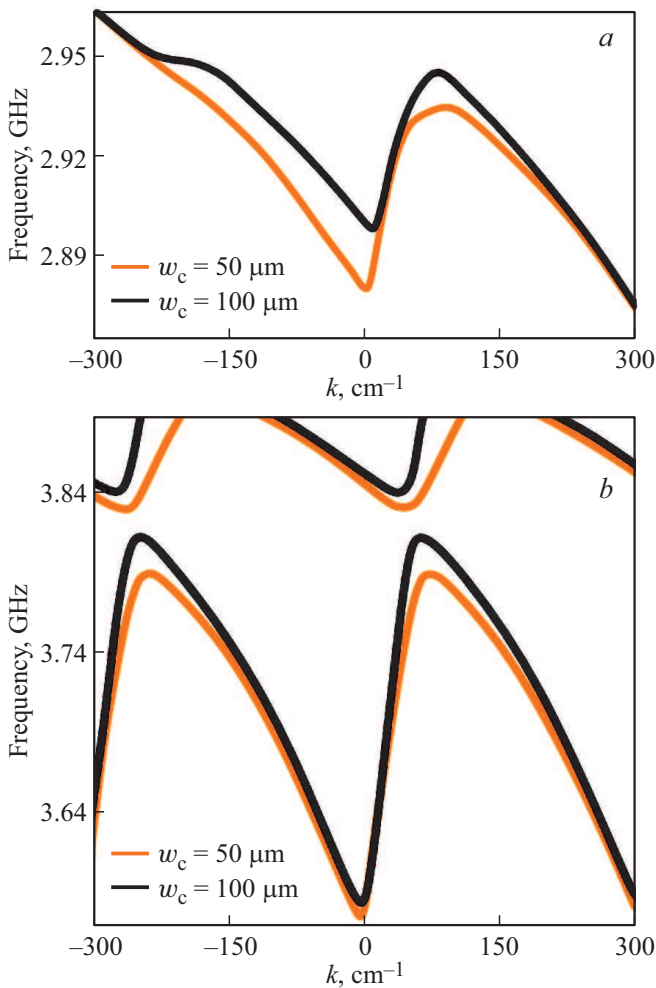


Figure 3. Dispersion curves calculated for the given structure with two various MC periods: *a*) low-frequency region of the dispersion curve, *b*) high-frequency region of the dispersion curve.

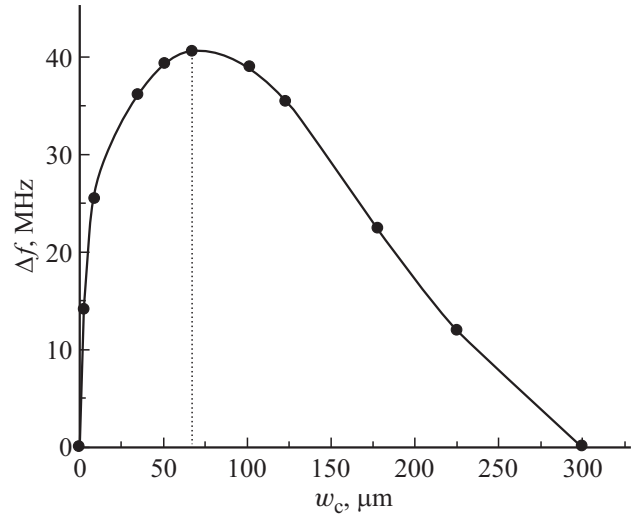


Figure 4. Frequency width of band gap 1 depending on the metallized plate width w_c .

$$\mu_{1,2}(\omega) = \frac{\omega_H(\omega_H + \omega_{M_{1,2}}) - \omega^2}{\omega_H^2 - \omega^2},$$

$$\mu_{a_{1,2}}(\omega) = \frac{\omega_{M_{1,2}}\omega}{\omega_H^2 - \omega^2},$$

where $\omega_{M_{1,2}} = \gamma 4\pi M_{1,2}$, $\omega_H = \gamma H_0$, $\gamma = 2\pi \cdot 2.8 \text{ MHz/Oe}$ is the gyromagnetic ratio in YIG film, $M_{1,2}$ is the saturation magnetization of each layer. For simulation of eigenwave propagation in a periodic structure, it is sufficient to consider one structure period that forms a MC lattice cell.

Dispersion curves were also calculated for SW propagating in the plus and minus y directions by solving the analytical equation from [22] for the non-periodic double-layer structure.

Dispersion curves calculated using the analytical method and finite element method are shown in Figure 2. Good agreement of one of the spin wave dispersion curve branches is observed, i.e. the branch that is in the negative wave number range. The opposite branch, however, differs greatly in the presence of a magnon-crystalline structure. Thus, the presence of a magnon-crystalline structure in the double-layer film not only adds band gaps into the wave spectrum, but also changes the dispersion curve angle and, as a consequence, the SW group propagation velocity.

Then dispersion curves were calculated for a one-dimensional magnon crystal with various filling ratios that was formed by periodic irregularities applied to one of the surfaces of the double-layer ferrite film, without considering the electromagnetic wave attenuation in ferrite. using the numeric simulation of the given structure, MSSW dispersion curves were built for structures with MC.

Figure 3, *a* and *b* show the dispersion curves: black curve — for MC with one-period width of the metallized plate $w_c = 100 \mu\text{m}$, orange curves — for MC with $w_c = 50 \mu\text{m}$. It can be seen that the effect of dispersion curve branch repulsion caused by the direct and

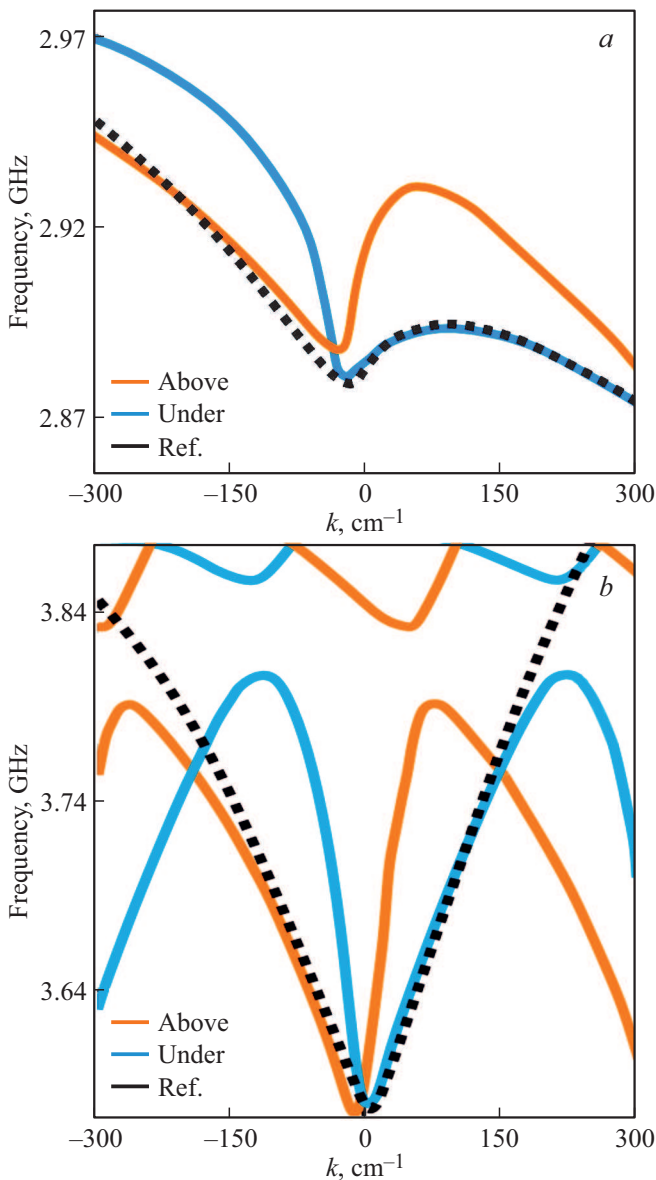


Figure 5. Dispersion curves calculated for the given structure with two various MC positions with respect to the YIG film: a) low-frequency region of the dispersion curve, b) high-frequency region of the dispersion curve.

back spin wave phase progression occurs in the LF region (Figure 3, a) for a branch in the negative wave number region. This effect becomes more pronounced with an increase in the filling ratio of the metallic structure near the wave-guiding structure surface. In the high-frequency range, this effect is minimized as shown in Figure 2.

To study the effect of the filling ratio of the metallic structure above the double-layer structure on the band gap frequency width, dispersion curves were calculated for the given structure with varied w_c .

When a metallized MC is added to the system, BG is formed, and when w_c increases to $70\ \mu\text{m}$, the BG width achieves its peak of $\Delta f = 40\ \text{MHz}$. The peak position is

marked by a vertical dotted line in Figure 4. With further increase in w_c to $w_c = L$, BG is closing gradually.

Figure 5, a and b show dispersion curves for the structure in Figure 1 with various MC positions with respect to the double-layer YIG film, i.e. above and below the film. The orange curve is a dispersion curve in case when MC is above the film with the lowest magnetization (M_1), blue curve is the case when MC is below the film with the highest magnetization (M_2) as shown in the detail in Figure 1, black dotted line is the magnetostatic surface wave dispersion for the double-layer film structure without metallization.

Depending on which side of the film MC is located, frequency shift of the dispersion curve branches and shift of the emerging band gaps take place. In case when MC is above the double-layer film (above YIG2), BG moves towards high wave numbers as can be seen in the high-frequency region in Figure 5, b; while in LF (Figure 5, a), the back wave also moves towards higher wave numbers (blue curves). When MC is placed near the film with high magnetization (YIG1), both the LF branch and BG in the high-frequency region move towards lower wave numbers.

4. Conclusion

Spin-wave signal propagation in a double-layer magnon microwaveguide with a metallic strip grid on the surface was studied in detail. nonreciprocity property of spin waves was examined by means of numeric simulation and eigenproblem solution. Transformation of dispersion curves of spin waves propagating in two opposite directions was detected. In addition, two frequency bands of spin wave propagation in magnon-crystalline double-layer structures were identified. The numeric simulation has shown that double-layer structures are capable of supporting two spin wave propagation frequency bands. And due to the presence of MC, band gaps occur on the surface in the high-frequency band. By varying the configuration and arrangement of the metallic strips on one of the film surfaces, band gap width and position in the spectrum and spin wave nonreciprocity properties may be controlled when the propagation direction is changed. The offered concept of double-layer magnon-crystalline structure may be used for the design of functional magnonics devices supporting frequency-selective multiband operation conditions.

Funding

The study was supported financially support by Russian Science Foundation grant No. 23-79-30027.

Conflict of interest

The authors declare that they have no conflict of interest.

References

- [1] S.A. Nikitov, A.R. Safin, D.V. Kalyabin, A.V. Sadovnikov, E.N. Beginin, M.V. Logunov, M.A. Morozova, S.A. Odintsov, S.A. Osokin, A.Yu. Sharaevskaya, Yu.P. Sharaevsky, A.I. Kirilyuk. *Phys.—Usp.* **63**, *10*, 945 (2020).
- [2] I.V. Vetrova, M. Zelent, J. Šoltys, V.A. Gubanov, A.V. Sadovnikov, T. Šcepka, J. Dérer, R. Stoklas, V. Cambel, M. Mruzckiewicz. *Appl. Phys. Lett.* **118**, *21*, 212409 (2021).
- [3] A.G. Veselov, S.L. Vysotsky, G.T. Kazakov, A.G. Sukharev, Yu.A. Filimonov. *Radiotekhnika i elektronika*, **39**, 2067 (1994). (in Russian).
- [4] N.M. Kozhevnikov. *Vliyaniye parametriceskikh spinovykh voln na dispersiyu i zatukhanie magnitostaticeskikh voln v plenkach zhelezotrievogo granata*. Dis. k.f.-m.n. Saratov. gos. un-ta im. N.G. Tchernyshevskogo, Saratov (2011). (in Russian).
- [5] A.G. Gurevich, G.A. Melkov. *Magnetization Oscillations and Waves*. CRC Press, London (1996).
- [6] A.A. Grachev, A.A. Martyshkin, S.E. Sheshukova, A.V. Sadovnikov, S.A. Nikitov. *Elektronika i mikroelektronika SVCh*, **1**, 387 (2019). (in Russian).
- [7] P.E. Zilberman, S.A. Nikitov, A.G. Timiryazev. *Pisma v ZhTF*, **42**, *3*, 82 (1985). (in Russian).
- [8] A.D. Boardman, S.A. Nikitov, N. Waby. *Phys. Rev. B* **48**, *18*, 13602 (1993).
- [9] M. Chen, M.A. Tsankov, J.M. Nash, C.E. Patton. *Phys. Rev. Lett.* **70**, *11*, 1707 (1993).
- [10] R.W. Damon, J.R. Eshbach. *J. Phys. Chem. Solids* **19**, *3–4*, 308 (1961).
- [11] T.W. O'Keeffe, R.W. Patterson. *J. Appl. Phys.* **49**, *9*, 4886 (1978).
- [12] S.N. Bajpai. *J. Appl. Phys.* **58**, *2*, 910 (1985).
- [13] M.A. Morozova, S.V. Grishin, A.V. Sadovnikov, D.V. Romanenko, Yu.P. Sharaevskii, S.A. Nikitov. *Appl. Phys. Lett.* **107**, *24*, 242402 (2015).
- [14] A.V. Chumak, P. Kabos, M. Wu, C. Abert, C. Adelman, A.O. Adeyeye, J. Akerman, F.G. Aliev, A. Anane, A. Awad, C.H. Back, A. Barman, G.E.W. Bauer, M. Becherer, E.N. Beginin, V.A.S.V. Bittencourt, Y.M. Blanter, P. Bortolotti, I. Boventer, D.A. Bozhko, S.A. Bunyaev, J.J. Carmiggelt, R.R. Cheenikundil, F. Ciubotaru, S. Cotofana, G. Csaba, O.V. Dobrovolskiy, C. Dubs, M. Elyasi, K.G. Fripp, H. Fulara, I.A. Golovchanskiy, C. Gonzalez-Ballester, P. Graczyk, D. Grundler, P. Gruszecki, G. Gubbiotti, K. Guslienko, A. Haldar, S. Hamdioui, R. Hertel, B. Hillebrands, T. Hioki, A. Houshang, C.-M. Hu, H. Huebl, M. Huth, E. Iacocca, M.B. Jungfleisch, G.N. Kakazei, A. Khitun, R. Khymyn, T. Kikkawa, M. Kläui, O. Klein, J.W. Kłos, S. Knauer, S. Koraltan, M. Kostylev, M. Krawczyk, I.N. Krivorotov, V.V. Kruglyak, D. Lachance-Quirion, S. Ladak, R. Lebrun, Y. Li, M. Lindner, R. Macêdo, S. Mayr, G.A. Melkov, S. Mieszczak, Y. Nakamura, H.T. Nembach, A.A. Nikitin, S.A. Nikitov, V. Novosad, J.A. Otálora, Y. Otani, A. Papp, B. Pigeau, P. Pirro, W. Porod, F. Porrati, H. Qin, B. Rana, T. Reimann, F. Riente, O. Romero-Isart, A. Ross, A.V. Sadovnikov, A.R. Safin, E. Saitoh, G. Schmidt, H. Schultheiss, K. Schultheiss, A.A. Serga, S. Sharma, J.M. Shaw, D. Suess, O. Surzhenko, K. Szulc, T. Taniguchi, M. Urbánek, K. Usami, A.B. Ustinov, T. van der Sar, S. van Dijken, V.I. Vasyuchka, R. Verba, S. Viola Kusminskiy, Q. Wang, M. Weides, M. Weiler, S. Wintz, S.P. Wolski, X. Zhang. *IEEE Trans. Magn.* **58**, *6*, 0800172 (2002). <https://doi.org/10.1109/TMAG.2022.3149664>
- [15] Iu.A. Iusipova. *Proc. Universities. Electronics* **24**, *2*, 160 (2019). (In Russ.).
- [16] P.V. Kuptsov. *Phys. Solid State* **65**, *6*, 903 (2023).
- [17] H. Suhl. *J. Phys. Chem. Solids* **1**, *4*, 209 (1957).
- [18] V.E. Demidov, M. Evelt, V. Bessonov, S.O. Demokritov, J.L. Prieto, M. Muñoz, J. Ben Youssef, V.V. Naletov, G. de Loubens, O. Klein, M. Collet, P. Bortolotti, V. Cros, A. Anane. *Sci. Rep.* **6**, 32781 (2016).
- [19] U.-H. Hansen, V.E. Demidov, S.O. Demokritov. *Appl. Phys. Lett.* **94**, *25*, 252502 (2009).
- [20] A.V. Sadovnikov, E.N. Beginin, M.A. Morozova, Yu.P. Sharaevskii, S.V. Grishin, S.E. Sheshukova, S.A. Nikitov. *Appl. Phys. Lett.* **109**, *4*, 042407 (2016).
- [21] S.A. Odintsov, E.G. Lökk, E.N. Beginin, A.V. Sadovnikov, *Russ. Technol. J.* **10**, *4*, 55 (2022). <https://doi.org/10.32362/2500-316X-2022-10-4-55-64>
- [22] S.A. Odintsov, S.E. Sheshukova, S.A. Nikitov, E.H. Lock, E.N. Beginin, A.V. Sadovnikov. *J. Magn. Magn. Mater.* **546**, 168736 (2022). ISSN 0304-8853

Translated by E.Ilnskaya